Faint M Dwarfs and the Structure of the Galactic Disk[1]

I. N. REID, J. E. GIZIS, J. G. COHEN, AND M. A. PAHRE

Palomar Observatory, 105-24, California Institute of Technology, Pasadena, California 91125
Electronic mail: inr@astro.caltech.edu, jeg@astro.caltech.edu, jlc@astro.caltech.edu, map@astro.caltech.edu

D. W. HOGG

Theoretical Astrophysics, 130-33, California Institute of Technology, Pasadena, California 91125
Electronic mail: hogg@tapir.caltech.edu

L. COWIE, E. HU, AND A. SONGAILA

Institute for Astronomy, University of Hawaii, 2680 Woodlawn Drive, Honolulu, Hawaii 96822
Electronic mail: cowie@ifa.hawaii.edu, acowie@ifa.hawaii.edu, hu@ifa.hawaii.edu

ABSTRACT. We use broadband photometry and low-resolution spectra of a complete sample of late-type K and M dwarfs brighter than $I=22$ in three fields at high galactic latitude to study issues relating to galactic structure and large-scale abundance gradients in the Galaxy. The observed starcounts in each field are a good match to the predictions of models based on deep starcount data in other intermediate-latitude fields, and these models identify the late-type stars as members of the Galactic disk. Abundances for these late-type stars are estimated via narrow-band indices that measure the strength of the TiO and CaH bands in their spectra. Our results show that the average abundance in the Galactic disk remains close to solar even at heights of more than 2 kpc above the Plane.

1. INTRODUCTION

It is by now generally agreed that the vertical distribution of stars in the Galactic disk cannot be represented by a simple, single-component density law. Deep, wide-field optical number–magnitude starcounts show that the slope of the overall density distribution flattens by a factor of ~ 4 between 1.2 and 1.5 kpc above the Plane, well before the halo becomes the dominant population at $z \sim 5$ kpc (Gilmore and Reid 1983; Majewski 1992; Reid and Majewski 1993—hereinafter, RM93; Gould et al. 1996). What is not clear, however, is how one interprets these "extra" stars, both in terms of deconvolving the observed distribution into thin and thicker components (Majewski 1993; Robin 1994) and in deciding the physical significance of the deconvolved components.

Majewski (1993) outlines eight different scenarios for the formation of what we will refer to as the intermediate population (or IP II), and one can characterize the extremes as being those models which treat the IP II as the result of a separate, distinct star-formation event (e.g., Wyse and Gilmore 1988; Robin et al. 1996) and those which identify the IP II as the high-velocity tail of the old disk (Norris 1987). One method of constraining these various hypotheses is through measurement of the abundance distribution of the stars in the IP II, in particular, determining whether there is a significant gradient in the mean abundance with height above the Galactic Plane. To date, however, the requisite observational data are still relatively sparse. Yoss et al. (1987) use observations of high-latitude K giants to derive a metallicity gradient of ~ -0.4 dex kpc^{-1} to z=700 pc. and ~ -0.18 dex kpc^{-1} thereafter (to 8 kpc), although their sample includes relatively few stars above 2.2 kpc and shows substantial dispersion. Trefzger et al. (1995) and Gilmore et al. (1995) have surveyed F and G dwarfs toward the South Galactic Pole, using VBLUW photometry and medium-resolution, low signal-to-noise spectra, respectively. Again, neither study includes many stars above 2.5 kpc. Trefzger et al. find a relatively steep gradient close to the Plane (~ -0.55 dex kpc^{-1}), and both match the K-giant survey in finding little variation in the mean abundance above ~ 1 kpc, although Gilmore et al.'s data show significantly more dispersion. Finally, Majewski's (1992) *UBV* data extend to $z > 10$ kpc and suggest a somewhat higher mean abundance below 6 kpc.

In this paper we present the first attempt to use observations of distant late-type K and M dwarfs to study this question. At least 80% of the stars in the Galactic disk are M dwarfs, so these stars have a high surface density at faint magnitudes. Moreover, M dwarfs can be recognized even with low dispersion spectra. At the faint magnitude level under consideration, any M star seen must be an M dwarf; high-luminosity M giants and supergiants would be so far out in the Galactic halo that even if they were to be found there in the same ratio as K giants and K supergiants (which is unlikely given the higher metallicity required to produce M giants), their surface density would be insignificant compared to the number of *bona fide* M dwarfs.
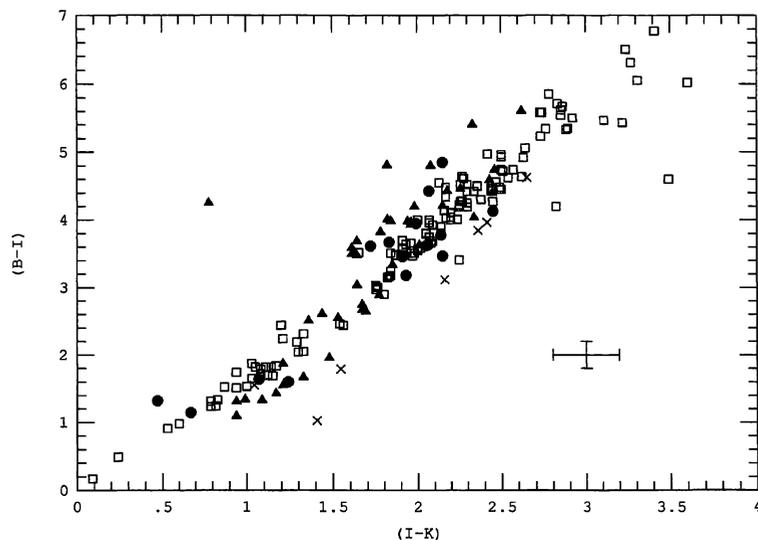
FIG. 1—The $(B - I)/(I - K)$ two-color diagram for stars in the 0-h field (solid dots), SSA 13 (crosses), and SSA 22 (solid triangles). The reference sequence is provided by Leggett's (1992) photometry of stars within 8 pc of the Sun (plotted as open squares). The error bar shows representative uncertainties for $I \sim 21$ magnitude and fainter.

Furthermore low-abundance M-type subdwarfs can be identified through the enhanced strength of the hydride bands (particularly CaH) relative to the TiO absorption (Bessell 1982). Until recently, the complex, diatomic-molecule dominated spectra of these stars defied quantitative abundance analysis, but Gizis (1997) has shown that the atmosphere models developed by Allard and Hauschildt (1995) can be combined with narrow-band spectrophotometry to derive an approximate ($\sim \pm 0.3$ dex) abundance scale for these stars. Given these results, we have undertaken a preliminary study, analyzing Keck LRIS data of a magnitude-limited sample of faint M dwarfs. Section 2 describes the observational data; Sec. 3 compares the observed color–magnitude diagrams against Galactic starcount models and discusses the abundance distribution; Sec. 4 summarizes our conclusions.

2. OBSERVATIONS

Our sample consists of the K and M dwarfs drawn from three fields: the 0-h deep field ($l = 125°$, $b = -50°$); SSA 13 ($l = 109°$, $b = 74°$); and SSA 22 ($l = 63°$, $b = -44°$). The first field is 7.3×2 arcmin in size (0.004 square degrees), while the other two fields are $6' \times 2'$ (0.003 sq. deg.). All three fields are part of a deep, K-band limited redshift survey being undertaken by groups at Caltech (Cohen et al. 1996) and Hawaii (Cowie et al. 1996). The primary goal is a deep redshift survey of extragalactic objects, but objects within the magnitude limits were observed irrespective of morphology. Here we concern ourselves with the Galactic stars found during the course of these redshift surveys. This paper discusses observations of the complete sample of 68 stars with $I < 22$ mag in these fields.

The spectroscopic sample consists of those objects with observed spectra judged to have sufficient signal-to-noise ratios to be useful in deducing abundances for these K and M dwarfs. It includes 43 stars. The spectroscopic observations

of the 0-h field sources are described in detail by Cohen et al. (1997), while Cowie et al. (1996) discuss the data for objects in the two Hawaii fields.

A detailed description of the observations and analysis of the $U,B,V,R,I,$ and K photometry for the 14 stars in the 0-h field can be found in Pahre et al. (1997). The same can be found for the Hawaii fields (observed only at B, I, and K) in Cowie et al. (1996). We have supplemented the SSA 22 data with BVI photometry obtained with LRIS on the Keck telescope in 1996 September, calibrating the observations using the same methods outlined by Pahre et al. (1997). These observations included shorter-exposure images, and hence avoided saturating the brighter stars. We have used the *IRAS* 100-μm maps to estimate the interstellar absorption in each field. Using the calibration given by Laureijs et al. (1994), we estimate a total extinction of $A_V \sim 0.22$ mag in the 0-h field, corresponding to $A_I \sim 0.10$, $E_{B-I} \sim 0.19$, and $E_{I-K} \sim 0.08$ mag; $A_V \sim 0.23$ mag in SSA 22; and negligible extinction ($A_V \sim 0.005$ mag) in SSA 13. We assume that all of the extinction lies in the immediate vicinity (within 200 pc) of the Sun. Figure 1 shows the reddening-corrected two-color $(B-I)/(I-K)$ diagram for all of the spectroscopically confirmed stars in these fields.

All of the objects were observed spectroscopically using multislit masks with LRIS (Oke et al. 1994) on the Keck 10-m telescope. The slits used were 1.4 arcsec wide, and a 300 1 mm^{-1} grating gives spectra of 16 Å (~ 5 pixels) resolution covering the wavelength range ~ 5000–10,000 Å. (The actual coverage on each spectrum depends on the exact position of the slit within the rectangular field.) Full details of the reduction procedures are given in Cowie et al. (1996) and in Cohen et al. (1997). The spectra from the 0-h field were set on a flux scale using observations of the white dwarf standard G191-B2B (Oke 1990). This star was observed using a 1.5-arcsec aperture longslit in LRIS. While the calibration takes out the overall spectral response of the CCD, vary-
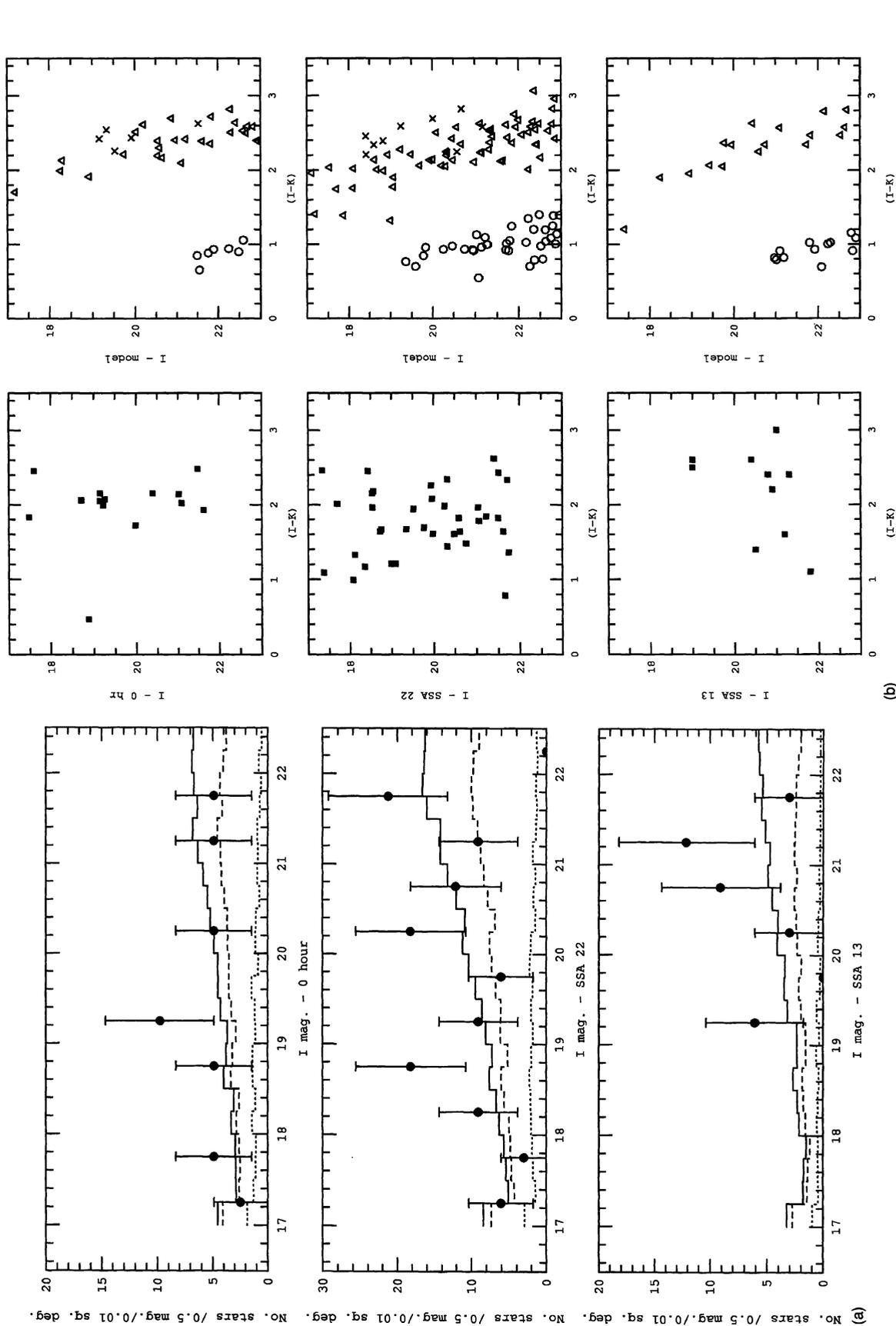
FIG. 2—(a) Predicted and observed number counts for the three fields in this study. The solid histogram outlines the total counts. The right-hand panel shows the predictions for each field (and for a solid angle of 0.01 square degrees) made by the model described in the text, where the red sequence is due to old disk (crosses) and IP II stars (triangles) and the blue due to halo stars (open circles). The left-hand panels plot the observed distributions.
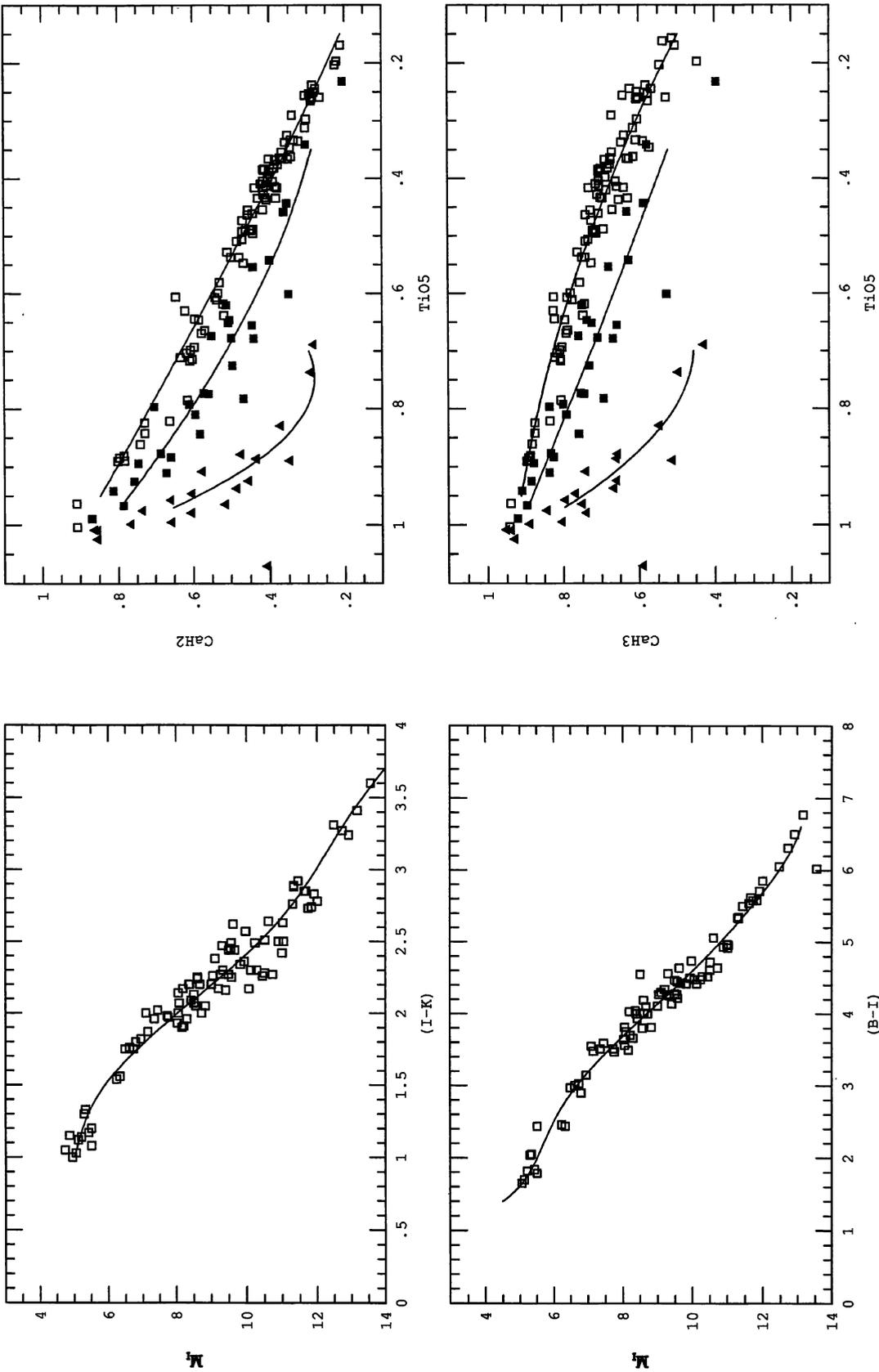
(b) Predicted and observed $(I, I - K)$ color–magnitude diagrams. The solid histogram outlines the total counts; the dotted line marks the contribution of the old disk; and the dashed line separates the contribution from the IP II and halo.

FIG. 4—Calcium hydride strength as a function of the TiO $\gamma(0,0)$ band strength. Data for single stars within 8 pc of the Sun (from RHG) are plotted as open squares. These define a solar-abundance sequence. The solid symbols are subdwarfs from Gizis (1997), with the squares being "normal" subdwarfs with [Fe/H] ~ -1 and the triangles "extreme" subdwarfs, [Fe/H] ~ -2. Second-order polynomials fitted to each sequence are also shown.

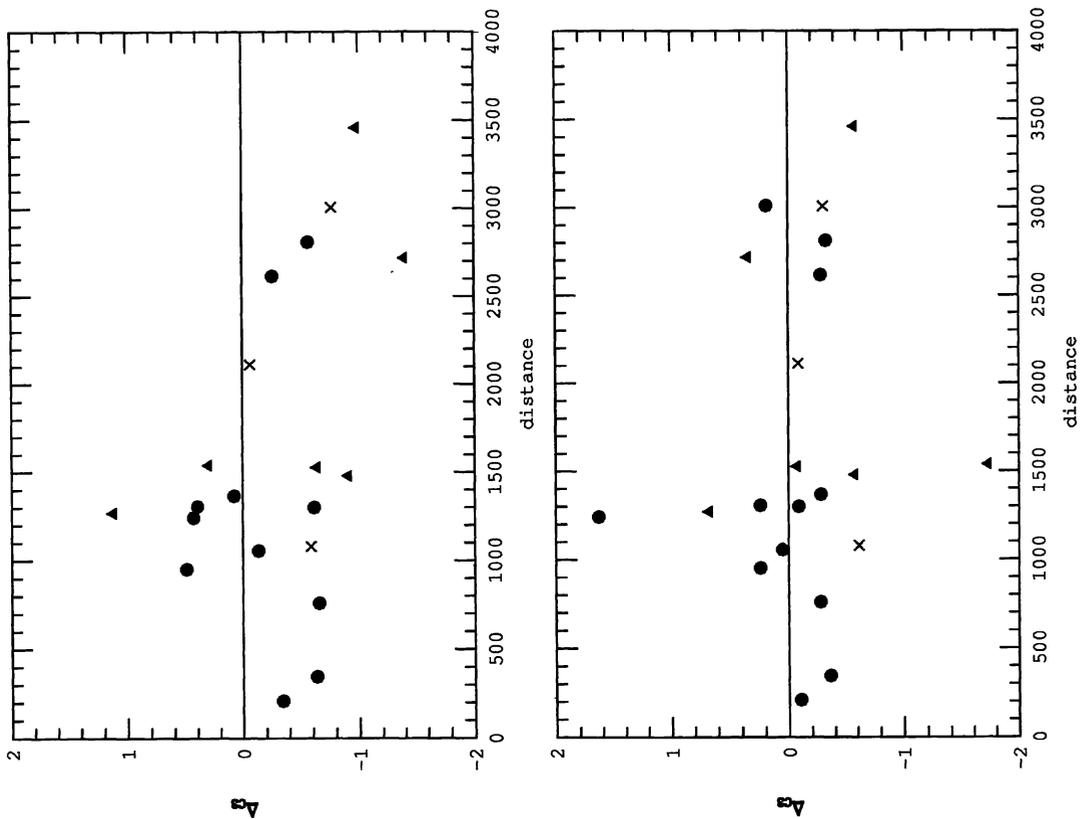FIG. 3—The $[M_I, (I - K)]$ and $[M_I, (B - I)]$ color-magnitude diagrams defined by stars within 8 pc of the Sun. The majority of the photometry is from Leggett (1992). In each case the line shows mean relation defined by a sixth-order polynomial fitted to the data.
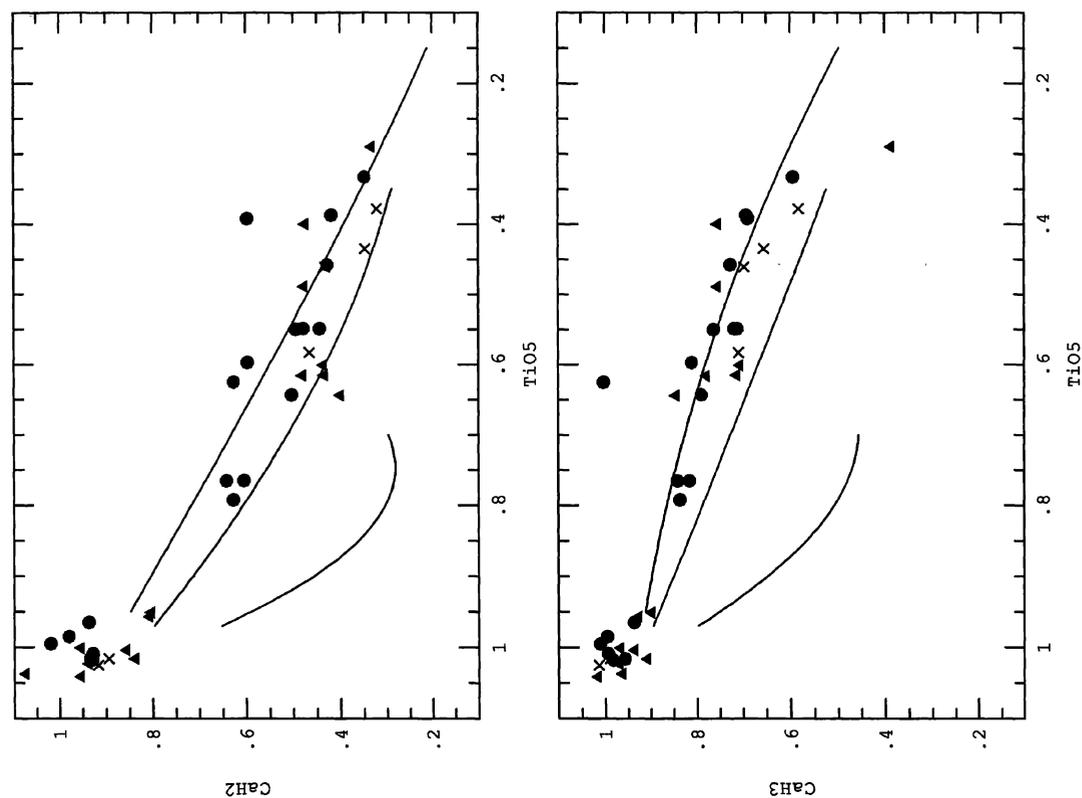
FIG. 5.—Calcium hydride and titanium oxide band strengths for the program stars in our sample. The data are coded as in Fig. 1 and the fiducial lines are the polynomial fits to the disk dwarfs, intermediate subdwarfs, and extreme subdwarfs from Fig. 4.

FIG. 6.—The normalized CaH indices, Δ_{C2} and Δ_{C3}, plotted against distance above (or below) the Galactic Plane.

TABLE 1
Spectroscopic Indices

Star	TiO$_5$	CaH$_2$	CaH$_3$
	0-h field		
PD0K 03	0.765	0.604	0.816
PD0K 04	0.792	0.627	0.837
PD0K 09	0.550	0.494	0.763
PD0K 16	0.643	0.503	0.790
PD0K 19	0.597	0.597	0.811
PD0K 21	0.458	0.428	0.726
PD0K 22	0.549	0.444	0.712
PD0K 49	0.387	0.419	0.693
PD0K 50	0.625	0.626	1.003
PD0K 91	0.549	0.479	0.718
PD0K 97	0.333	0.348	0.594
PD0K 101	0.392	0.597	0.689
	SSA 13		
17	0.461	0.433	0.697
35	0.435	0.347	0.655
73	0.417	0.508	0.808
84	0.378	0.321	0.583
97	0.583	0.466	0.709
	SSA 22		
24	0.290	0.333	0.387
61	0.644	0.400	0.845
112	0.400	0.475	0.754
157	0.489	0.477	0.755
169	0.615	0.435	0.713
171	0.601	0.436	0.706
200	0.616	0.480	0.779

ing losses of light at the slit lead to the calibrations for individual multislits being uncertain by up to 10% over broad wavelength intervals of ~2000 Å or more. However, the widest of our narrow-band indices spans only 250 Å, so the uncertainties in the indices are dominated by the signal to noise in the individual spectra rather than by systematic errors in the flux calibration.

3. DISCUSSION

3.1 Starcounts

We have compared the observed color–magnitude distribution of the photometric sample of 68 stars with $I < 22$ mag against the predictions of starcount models. As the starting point for our analysis, we take model B from Reid et al. (1996—hereinafter RYMTS). This model includes three stellar components: the old disk, modeled as a sech$^2(h/h_0)$ distribution, with h_0 of 350 pc; an intermediate population, with a local normalization of 5% relative to the old disk and a sech^2 density law, $h_0 = 1500$ pc; and an $r^{-3.5}$ halo with the local density normalized to 0.15% that of the old disk. We have also adopted a scale length of 2.5 kpc for the radial density law in the Galactic disk (Robin et al. 1992). The color–magnitude relations adopted for these three populations are from photometry of nearby stars, of members of the open cluster NGC 2420, and of stars in the globular cluster NGC 6752, respectively. Full details are given in RYMTS, who show that this model reproduces both the color–

magnitude distribution in the intermediate-latitude PSR 1640 field ($l = 41°$, $b = 38°$) and the density distribution toward the South Galactic Pole.

Figure 2(a) compares the overall starcount predictions of model B against the observations in the three fields considered in this paper. The agreement is well within the formal Poissonian uncertainties. Limiting the sample to the magnitude range $17 < I < 22$, we observe 19, 11, and 37 stars in the 0-h field, SSA 13 and SSA 22. The predicted number counts are 15, 11, and 32 stars in the respective fields.

Figure 2(b) compares the color–magnitude distributions predicted by this model against the observed $[I, (I - K)]$ distribution in each field. For greater clarity, the predicted starcounts in each field are matched to a solid angle of 0.01 square degrees—a factor of 2.5 greater than the 0-h field and ~3 greater than the SSA 13 and SSA 22. The model predicts two distinct sequences: late F- and G-type halo subdwarfs $[(I - K) < 1.5]$ lying at a distance of ~10 kpc and a sequence of late-K and M-type disk dwarfs, mainly contributed by the IP II, at distances of from ~1 to 4 kpc. The small scale height of the old disk component leads to a low surface density and an insigificant contribution to these faint starcounts, even in the intermediate-latitude field SSA 22.

As described in RYMTS, the convolution of the density law and the sampling volume lead to a preferred distance modulus for a given stellar populaton. Since the old disk has the steepest vertical density law and the halo the shallowest, the former stars are sampled primarily at $(m - M) \sim 7$ mag, while the latter lie preferentially at $(m - M) \sim 15$ mag. Thus, at a given apparent magnitude, the halo contributes more luminous (bluer) stars than the disk. The models plotted in Fig. 2(b) clearly show that the later-type stars, which contribute the bulk of the stars in each field, are members of the Galactic disk.

3.2 The Abundance Distribution

The primary aim of this paper is to use the late-type dwarfs in our sample to probe the abundance distribution at large distances above the Plane. In order to do this we need to estimate both abundances and distances. We have used B-, I-, and K-band data for individual stars within 8 pc to define $[M_I, (B-I)]$ and $[M_I, (I-K)]$ relations (Fig. 3). The curves fitted are sixth-order polynomials, and the dispersion is $\sigma_I = 0.35$ magnitudes in the $(B-I)$ calibration and $\sigma_I = 0.52$ mag for $(I-K)$. Comparing the distance estimates for individual stars, the mean difference between the $(B - I)$ and $(I-K)$ photometric parallaxes is 40% of the distance based on averaging the two estimates, with no evidence of a systematic offset between the two distance scales. We have therefore taken the straight average of the two estimates as the appropriate distance for each star and adopt an uncertainty of ~30%. This is adequate for the present purposes.

Gizis (1997) has shown that abundance estimates for late-K and M-type dwarfs can be derived from the relative strengths of the calcium hydride band at ~6800 Å and the titanium oxide $\gamma(0,0)$ band at ~7050 Å. Reid et al. (1995—RHG) have defined several narrow-band indices designed to measure the strengths of these bands, and Fig. 4 plots data

for two of the CaH indices against TiO$_5$, the full depth of the TiO bandhead. In addition to data (from RHG) for single disk stars within 8 pc of the Sun, we have plotted Gizis' measurements of the band strength in intermediate and extreme subdwarfs. A comparison with the Allard and Hauschildt models shows that the former stars, plotted as solid square in Fig. 4, have an abundance of [Fe/H]~-1 while the latter are significantly more metal poor, with [Fe/H]~-2. We have taken nearby K and M dwarfs to be representative of a solar-abundance population.

We have fitted second-order polynomials to each of the three sets of stars in Fig. 4 and used these as a grid to match against narrow-band indices derived from our observations of the faint program stars. Table 1 lists the band-strength data for the later-type stars in the current sample. Broadband photometry and positions for stars in SSA 13 and SSA 22 are given by Cowie et al. (1996), while Pahre et al. (1997) present *UBVRIK* for stars in the 0-h field. Figure 5 plots the resulting band strengths and it is clear that the IP II stars in our sample lie closest to the polynomial fit to the local (solar-abundance) stars, consistent with previous observations of IP II F and G dwarfs. We have attempted to set our abundance estimates onto a more quantitative scale by using the [Fe/H]=0 (nearby stars) and [Fe/H]=-1 (intermediate subdwarfs) sequences as fiducial references. Defining CaH^0 and CaH^{-1} as the values predicted by the solar and [Fe/H]=-1 relations for a given band strength, TiO$_5$, we calculate the quantity

$$\Delta_C=\frac{CaH^{obs}-CaH^0}{CaH^0-CaH^{-1}},$$

where CaH^{obs} is the observed strength of the CaH feature for the star in question. This scaling compensates for the changing separations of the two fiducial sequences, although without an adequate number of calibrators with high-precision abundance measurements, we can only assume that the variation in Δ_C with [Fe/H] is similar throughout the full temperature range covered here.

Using the distances derived from the average of the photometric parallaxes, we have computed the distance, z, above the Galactic Plane for each star. Limiting the sample to stars with significant TiO absorption (TiO$_5<0.85$), Fig. 6 plots the scaled CaH indices against z. The average values of the two indices if we include all stars are $\Delta_{c2}=-0.16$ and $\Delta_{c3}=-0.06$ (24 stars), while we derive $\Delta_{c2}=-0.27$ and $\Delta_{c3}=-0.06$ for the 15 stars with $z<2000$ pc. As yet, we do not have sufficient calibrating observations of stars of known abundance to be able to transform these measured offsets into real abundances, but the present results are clearly suggestive of values closer to those of the old disk than previously suggested.

4. CONCLUSIONS

We have analyzed photometry and low-resolution spectroscopy of faint late-K and early-M dwarfs in three intermediate- and high-latitude fields. A comparison with the predictions of a starcount model which matches the faint ($R<24$) stellar color–magnitude distribution in two other fields (Reid et al. 1996) shows that these stars lying at distances of up to 2 kpc above the Plane and members of the intermediate population. Our analysis, based on the strength of CaH and TiO molecular bands, demonstrates that these stars have abundances close to that of the old disk. Clearly, these results are preliminary, both given the total number of stars in our sample and the approximate nature of the calibration of the measured band strength against real abundances. However, our analysis does indicate a new possible direction that can be taken in exploring the abundance distribution within Galactic stellar populations.

REFERENCES

Allard, F. and Hauschildt, P. H. 1995, ApJ, 445, 433
Bessell, M.S. 1982, Proc. Astron. Soc. Australia, 4, 417
Cohen, J. G., Hogg, D. W., Pahre, M. A., and Blandford, R. 1996, ApJ, 462, L9
Cohen, J. G., et al. 1997, in preparation
Cowie, L. L., Songaila, A., Hu, E. M., and Cohen, J. G. 1996, AJ, 112, 839
Gilmore, G. and Reid, N. 1983, MNRAS, 202, 1025
Gilmore, G. F., Wyse, R. F. G., and Jones, J. B. 1995, AJ, 109, 1095
Gizis, J. E. 1997, AJ, 113, 806
Gould, A., Bahcall, J. N., Flynn, C. 1996, ApJ, 465, 759
Laureijs, R. J., Helou, G., and Clark, F. O. 1994, in First Symposium on the Infrared Cirrus and Diffuse Interstellar Clouds, ASP Conf. Ser. 58, 133, ed. R. M. Cutri and W. B. Latter
Leggett, S. K. 1992, ApJS, 82, 351
Majewski, S. R. 1992, ApJS, 78, 87
Majewski, S. R. 1993, ARAA, 31, 575
Norris, J. 1987, AJ, 93, 616
Oke, J. B. 1990, AJ, 99, 1621
Pahre, M. A., et al. 1997, in preparation
Reid, N. and Majewski, S. R. 1993, ApJ, 409, 635 (RM93)
Reid, I. N., Hawley, S. L., and Gizis, J. E. 1995, AJ, 110, 1838 (RHG)
Reid, I. N., Yan, L., Majewski, S. R., Thompson, I., and Smail, I. 1996, AJ, 112, 1472 (RYMTS)
Robin, A. C., Crézé, M., and Mohan, V. 1992, A&A, 265, 32
Robin, A. C. 1994, Astronomy from Wide-field Imaging, IAU Symposium 161, ed. H. T. MacGillivray et al. (Dordrecht, Kluwer Academic), p. 403
Robin, A. C., Haywood, M., Crézé, M., Ojha, D. K., and Bienaymé, O. 1996, A&A, 305, 125
Trefzger, Ch. F., Pel, J. W., and Gabi, S. 1995, A&A, 304, 381
Wyse, R. F. G., and Gilmore, G. F. 1988, AJ, 95, 1404
Yoss, K. M., Neese, C. L., and Hartkopf, W. I. 1987, AJ, 94, 1600